JARO (2017)
DOI: 10.1007/s10162-017-0631-y

JARO
Journal of the Association for Research in Otolaryngology

Research Article

Structural and Ultrastructural Changes to Type I Spiral Ganglion Neurons and Schwann Cells in the Deafened Guinea Pig Cochlea

Andrew K. Wise,[1,2,4] Remy Pujol,[1,3] Thomas G. Landry,[1] James B. Fallon,[1,2,4] and Robert K. Shepherd[1,2]

[1]*The Bionics Institute, 384-388 Albert Street, East Melbourne, Victoria 3002, Australia*

[2]*Department of Medical Bionics, University of Melbourne, Melbourne, Australia*

[3]*INSERM Unit 1051, INM, Montpellier, France*

[4]*Department of Otolaryngology, University of Melbourne, Melbourne, Australia*

Received: 27 June 2016; Accepted: 21 June 2017

ABSTRACT

Sensorineural hearing loss is commonly caused by damage to cochlear sensory hair cells. Coinciding with hair cell degeneration, the peripheral fibres of type I spiral ganglion neurons (SGNs) that normally form synaptic connections with the inner hair cell gradually degenerate. We examined the time course of these degenerative changes in type I SGNs and their satellite Schwann cells at the ultrastructural level in guinea pigs at 2, 6, and 12 weeks following aminoglycoside-induced hearing loss. Degeneration of the peripheral fibres occurred prior to the degeneration of the type I SGN soma and was characterised by shrinkage of the fibre followed by retraction of the axoplasm, often leaving a normal myelin lumen devoid of axoplasmic content. A statistically significant reduction in the cross-sectional area of peripheral fibres was evident as early as 2 weeks following deafening ($p < 0.001$, ANOVA). This was followed by a decrease in type I SGN density within Rosenthal's canal that was statistically significant 6 weeks following deafening ($p < 0.001$, ANOVA). At any time point examined, few type I SGN soma were observed undergoing degeneration, implying that once initiated, soma degeneration was rapid. While there was a significant reduction in soma area as well as changes to the morphology of the soma, the ultrastructure of surviving type I SGN soma appeared relatively normal over the 12-week period following deafening. Satellite Schwann cells exhibited greater survival traits than their type I SGN; however, on loss of neural contact, they reverted to a non-myelinating phenotype, exhibiting an astrocyte-like morphology with the formation of processes that appeared to be searching for new neural targets. In 6- and 12-week deafened cochlea, we observed cellular interaction between Schwann cell processes and residual SGNs that distorted the morphology of the SGN soma. Understanding the response of SGNs, Schwann cells, and the complex relationship between them following aminoglycoside deafening is important if we are to develop effective therapeutic techniques designed to rescue SGNs.

Keywords: spiral ganglion neuron, Schwann cell, deafness, nerve degeneration, nerve regeneration, cochlear implant

INTRODUCTION

Spiral ganglion neurons (SGNs), the afferent axons of the auditory nerve, convey acoustic information from the hair cells of the cochlea to the central auditory pathway. There are two SGN populations in mammalian cochleae: type I SGNs exclusively innervating

Correspondence to: Andrew K. Wise · The Bionics Institute · 384-388 Albert Street, East Melbourne, Victoria 3002, Australia. Telephone: +61 3 9667 7500; email: awise@bionicsinstitute.org

Published online: 17 July 2017

inner hair cells (IHCs) and type II SGNs innervating outer hair cells (OHCs). These SGNs exhibit clear morphological features that distinguish the two cell types: (i) Type I SGNs exhibit a large soma containing a spherical nucleus with a pronounced nucleolus, slightly myelinated by a satellite Schwann cell, a cytoplasm rich in ribosomes with few neurofilaments, and highly myelinated peripheral and central fibres and (ii) type II SGNs have a small soma ensheathed by a non-myelinating Schwann cell, a cytoplasm containing large numbers of neurofilaments and few ribosomes, with unmyelinated peripheral and central fibres (Kimura et al. 1979; Spoendlin and Schrott 1989; Anniko et al. 1995). In the guinea pig, the myelinated type I SGNs have a soma area of ~200 μm^2 and represent >90 % of all SGNs while the unmyelinated type II SGN is considerably smaller (100 μm^2) and represents <10 % of the SGN population (Morrison et al. 1975; Brown 1987b).

The type I SGN contains two types of myelin laid down under different glial cell types. The glial limitans, located within the internal auditory meatus, contains a clear transition between peripheral and central myelin (Toesca 1996; Hurley et al. 2007). Peripheral myelin, laid down by Schwann cells, is associated with the peripheral fibres, the soma, and the peripheral portion of the central process, while central myelin, laid down by oligodendrocytes, includes that portion of the type I axon central to the glial limitans (Toesca 1996; Knipper et al. 1998; Hurley et al. 2007).

Sensorineural hearing loss is the most common cause of deafness and typically results from damage to the sensory hair cells of the cochlea. This form of hearing loss can be caused by many factors including exposure to ototoxic drugs such as the aminoglycosides (Forge and Schacht 2000), or exposure to loud noise, although noise exposure can also initiate damage at the terminal endings of type I SGNs (Kujawa and Liberman 2015). A direct consequence of ototoxically induced damage to or loss of neural contact with the IHC is the anterograde degeneration of the type I SGN. A major factor contributing to type I SGN degeneration is the loss of the endogenous trophic support normally provided by the hair cells (Ylikoski et al. 1993; Schecterson and Bothwell 1994; Tan and Shepherd 2006) and supporting cells (Stankovic et al. 2004; Zilberstein et al. 2012) of the organ of Corti. Type I SGN degeneration is progressive over time with as few as 5–15 % of neurons remaining following extended periods of severe-profound sensorineural hearing loss (Spoendlin 1975; Webster and Webster 1981; Leake and Hradek 1988; Xu et al. 1993; Shepherd and Javel 1997; Hardie and Shepherd 1999; Ladrech et al. 2004). The rate of type I SGN degeneration varies among species and aetiology; however, in general, degeneration occurs rapidly in guinea pigs (weeks; (Webster and Webster 1981; Wise et al. 2005), Shepherd et al. 2005), compared to cats (months; Leake and Hradek 1988; Fallon et al. 2014) and humans (years; (Nadol et al. 1989).

The SGNs are the primary target cells for cochlear implants that function by electrically stimulating the residual neural population to provide auditory perception to recipients with few, if any, residual hair cells. However, extensive SGN degeneration may negatively impact on the clinical efficacy of cochlear implants (Seyyedi et al. 2014). It is important to understand the response of SGNs following deafness as these findings will impact on strategies designed to protect and regenerate these neurons (Shepherd et al. 2005; Wise et al. 2005; Glueckert et al. 2008; Atkinson et al. 2012; Leake et al. 2013; van Loon et al. 2013; Gillespie et al. 2014; Pinyon et al. 2014). Moreover, given the key role that Schwann cells are known to play in peripheral nerve repair (Glenn and Talbot 2013; Jessen and Mirsky 2016), it is equally important to understand the response of cochlear Schwann cells during anterograde degeneration of type I SGNs.

The aim of this study was to describe the ongoing ultrastructural changes in type I SGNs and Schwann cells in guinea pigs over a course of 12 weeks following deafening with aminoglycoside drugs. We selected to evaluate type I SGNs because they form the great majority of afferent neurons within the auditory nerve; they are readily identifiable and are the target neurons for stimulation via a cochlear implant.

MATERIALS AND METHODS

Animals

Adult pigmented Dunkin–Hartley guinea pigs of either sex were used in the study ($n = 14$). All animals had otoscopically normal tympanic membranes. The experimental procedures were approved by the Animal Research Ethics Committee of the Royal Victorian Eye and Ear Hospital in accordance with the National Institutes of Health Guidelines for the Care and Use of Laboratory Animals and conformed to the Code of Practice of the National Health and Medical Research Council of Australia.

Auditory Brainstem Responses

Auditory brainstem responses (ABRs) were measured to assess the hearing status of the guinea pigs prior to and following deafening, using procedures described previously (Richardson et al. 2005; Wise et al. 2010).

Briefly, guinea pigs were anaesthetised with ketamine (60 mg/kg, Parnell Australia) and xylazine (4 mg/kg, Ilium, Australia) via intramuscular administration and placed on a heat pad with the temperature maintained at 37 °C in a sound attenuated room. ABRs were measured to acoustic clicks delivered by a calibrated speaker at intensities up to 100 dB peak equivalent (p.e.) sound pressure level (SPL). The amplified ABR was recorded and averaged over 200 trials using stimulus intensities ranging from 10 to 100 dB p.e. SPL. Threshold was determined for all guinea pigs prior to deafening (Wise et al. 2010) and only animals with normal hearing thresholds in both ears (ABR threshold <50 dB p.e. SPL) were used in the study.

Deafening

Three guinea pigs were used as normal hearing controls while 11 animals were deafened using the ototoxic aminoglycoside kanamycin and the loop diuretic frusemide (Gillespie et al. 2003; Wise et al. 2010). Briefly, each guinea pig was anaesthetised with isoflurane (4 % induction, 1–2 % maintenance) in O_2 (1–1.5 L/min). The right jugular vein was cannulated, and frusemide (130 mg/kg; Ilium, Australia) diluted in 2.5 mL warm Hartmann's solution was slowly injected. Kanamycin sulphate (420 mg/kg; Sigma-Aldrich, USA) dissolved in 3 mL Hartmann's solution was injected subcutaneously. Deafness durations of 2, 6, and 12 weeks were used. The hearing status of each guinea pig was reassessed 1 week after deafening by measuring ABRs as described above. All deafened guinea pigs exhibited a bilateral increase in the click-evoked ABR threshold of at least 50 dB.

Fixation and Histological Preparation

Following the specified deafness duration, each guinea pig was anaesthetised (ketamine, 60 mg/kg, and xylazine, 4 mg/kg; i.m.), and both cochleae were exposed. The round and oval windows were opened and a small hole was created in the apex of the cochlea to enable intracochlear fixation (Puel et al. 1994). A cannula was positioned at the opening of the round window and 2 mL of 3.5 % glutaraldehyde in 4 °C phosphate buffered saline (PBS) was slowly perfused through the cochlea. Following local cochlear perfusion, each guinea pig was euthanised (150 mg/kg sodium pentobarbital intraperitoneal; Virbac Pty. Ltd., Australia) and perfused transcardially with warm saline containing 0.025 % (*w*/*v*) sodium nitrite and 0.1 % (*v*/*v*) heparin sodium, followed by 4 % paraformaldehyde and 2.5 % glutaraldehyde in 4 °C PBS. The temporal bones were removed and placed in 3.5 % glutaraldehyde in PBS for 2 h at room temperature, followed by 2 h in osmium tetroxide (1 % OsO_4 and 0.8 % K_4FeCN_6) in the dark on a rotation plate at room temperature. The tissue was then decalcified in a solution containing 10 % (wt/vol) ethylenediamine tetraacetic acid (EDTA) in 0.1 M PBS, dehydrated, and embedded in Spurr's resin.

The resin-embedded cochleae were bisected in the midmodiolar plane and a half-turn surface preparation of the lower basal turn was isolated from the remaining cochlea (Fig. 1a). The basal half-turn was then further cut into two quarter-turns (regions 1 and 2, Fig. 1b) and two blocks in two different orientations (transverse and longitudinal) were cut for each region. The longitudinal blocks were further divided into two smaller blocks (Fig. 1c) to produce 'distal' and 'medial' blocks. All blocks were then re-embedded in resin. Ultra-thin (80–100 nm) and semi-thin (1 μm) sections were collected from the longitudinal and transverse blocks. Ultra-thin sections were mounted on copper mesh grids and stained with 1.5 % uranyl acetate in 70 % ethanol for 35 min. Semi-thin sections were mounted on glass slides and stained with Toluidine Blue. Each grid of ultra-thin sections was separated by approximately 24 μm to ensure ultrastructural analysis at different locations. Four to eight grids were taken from each block. The sections were examined with a JEM-1011 electron microscope (JEOL, Japan).

Histological Analysis

Organ of Corti Status Observations of the status of the organ of Corti were made in transverse sections with particular focus on the region of the habenula perforata (Fig. 1c). Although no quantitative data was collected, qualitative assessment of hair cell and the peripheral nerve fibre survival were made in order to assess of the status of the organ of Corti in cochlear regions under examination.

Light Microscopy: Spiral Ganglion Neuron Cell Body Analysis Four midmodiolar transverse sections (1 μm thick with a minimum 24 μm separation to ensure each SGN is only counted once) from each cochlea were stained with Toluidine Blue for general histological examination. The density measurements of type I SGNs were performed by a single observer blinded to the deafness duration of each sample. Sections were viewed and imaged using an Axioplan inverted microscope and Axioplan software (Zeiss, Germany). For each section, a 20× magnification brightfield image (442 × 331 μm) of Rosenthal's canal was taken. The periphery of Rosenthal's canal was outlined (excluding the intraganglionic spiral bundle) and its cross-sectional area determined using ImageJ V1.46 (NIH, USA, http://rsb.info.nih.gov/ij/index.html, RRID:nif-0000-30467). Type I SGNs were

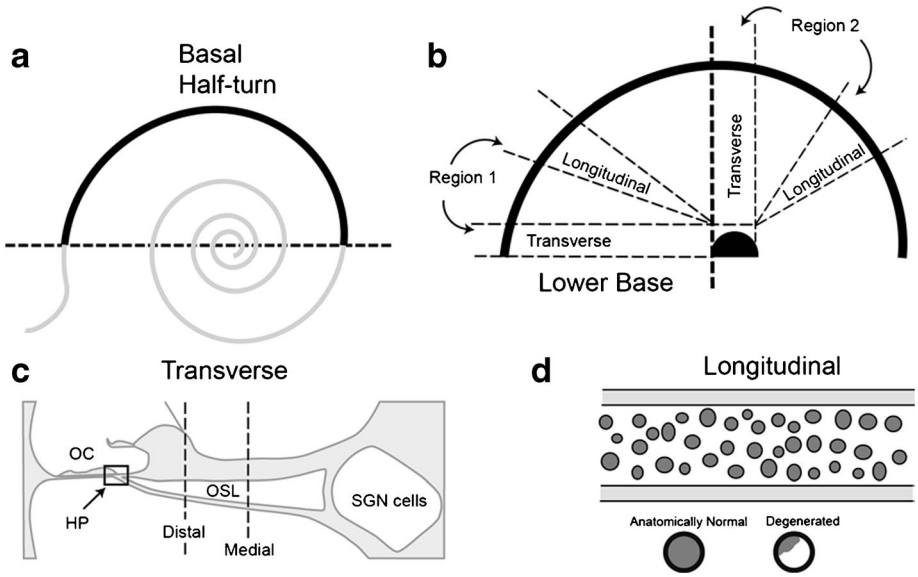

FIG. 1. Schematic diagram of the histological sectioning used for SGN and peripheral fibre analysis. **a** The resin-embedded cochlea was bisected down the midline (*dotted line*) and the basal half-turn was removed (*thick black line*). All analysis was carried out on the basal half-turn only. **b** The basal half-turn was further divided into two regions (regions 1 and 2). A thick block (~1 mm) was cut in the 'transverse' plane in each of the two regions. A wedge-shaped 'longitudinal' block was then cut for the cross-sectional analysis of the peripheral fibres. **c** Nerve and residual cells in the organ of Corti (*OC*), at the habenula perforata (*HP*) within the osseous spiral lamina (*OSL*), and SGN cell bodies (located in Rosenthal's canal) were examined in transverse sections. **d** Longitudinal blocks were cut at a distal or medial OSL position to obtain OSL cross sections that were used in analysis of the peripheral fibres as indicated in the schematic representation of a longitudinal OSL cross section. Peripheral fibre analysis involved measuring the area of the fibre axoplasm within the myelin sheath and categorisation of each fibre as anatomically normal or degenerated based on whether the area of the axoplasm occupied greater or less than 90 % of the myelin lumen (see schematic examples of these fibres).

identified by the presence of a large soma containing a spherical nucleus with a pronounced nucleolus, and myelinated peripheral and central fibres. Only type I SGNs that exhibited a clear nucleus and nucleoli were counted. In addition, the soma area of ten randomly selected SGNs per section was measured by tracing the outer perimeter of the cell body using the same software package. The SGNs were selected by randomly generated *x*-*y* coordinates. A grid was mapped onto the image and a random number generator was used to generate *x* and *y* values. If these coordinates fell within the confines of Rosenthal's canal, the neuron closest to the coordinate was selected.

Transmission Electron Microscopy: Analysis and Quantification of Spiral Ganglion Neurons and Their Peripheral Fibres

To quantify the SGN peripheral fibre ultrastructure, a series of longitudinal 15,000× transmission electron microscopy (TEM) images were taken at both the distal and medial sites of the two cochlear regions (Fig. 1b, c). Six fibres in each of these images were randomly selected. Peripheral fibres were selected by randomly generated *x*-*y* coordinates. A grid was mapped onto the image and a random number generator was used to generate *x* and *y* values. If these coordinates fell within the osseous spiral lamina (OSL) confines, the fibre closest to the coordinate was selected.

The cross-sectional areas of the myelin sheath lumen (i.e. the area within the myelin sheath) and the area occupied by the peripheral fibre axoplasm were calculated for each fibre using ImageJ (Fig. 1d). Fibre area measurements were carried out semi-automatically whereby pixel shade thresholding was used to automatically distinguish between the myelin sheath, fibre axoplasm, and empty space, although some manual outlining was usually necessary. A correction procedure (Romero et al. 2000) was used to adjust for slight differences in sectioning angle between sections as sectioning angles more oblique to the cross-sectional plane of the fibre would create larger area measurements. Here, eight representative fibres in each cochlear sample were analysed in the low magnification map images to estimate the sectioning obliqueness. The average ratio of the major to minor length axes of the outer myelin sheath was determined for these fibres, and all area measures from that sample were normalised to that value. This normalisation converts any elliptical elongation to the circular equivalent to normalise fibre area between samples. The percentage of the lumen space occupied by the axoplasm was measured, and anatomically

normal fibres were defined as having an axoplasm content occupying over 90 % of the myelin lumen and degenerating fibres were defined as having axoplasm occupying less than 90 % of the lumen (Fig. 1d).

Peripheral fibre densities were also determined at both the distal and medial sites of the OSL for the two cochlear regions (1 and 2: Fig. 1c). Five of the 15,000× magnification images were randomly selected and measurements were made of the density of 'anatomically normal' and 'degenerating' fibres that were entirely captured in the 55.8μm^2 images and averaged over the five images. Average fibre density was determined for the four cochlear regions (regions 1 and 2; distal and medial OSL location). A requirement of this analysis was that only complete fibre profiles were measured (i.e. only profiles in which the entire myelin lumen was visible in the image were included). Consequently, there was a slight bias of higher fibre density for smaller fibres observed in the deafened cochlea than otherwise would be if fibres in all groups were the same size, as smaller fibres would be more likely to have myelin lumen completely visible in the map.

Statistical Analysis

Peripheral fibre and SGN morphology were examined statistically by comparing the duration of deafness (control, 2, 6, and 12 weeks), cochlear region, and distal/medial location within the OSL (Fig. 1). A one way analysis of variance (ANOVA) on ranks was used for analysis of non-parametric data while a three-way analysis of variance (ANOVA), and a Holm–Sidak post hoc analysis was used for normally distributed data.

RESULTS

The gross light microscope changes observed over the 12-week post-deafening period used in the present study are illustrated in Figure 2. The progressive deafness-induced changes in the organ of Corti, OSL, and Rosenthal's canal are apparent when compared with the normal control cochlea (Fig. 2a). The detailed results below are based on TEM analysis of cochlear tissue. The results presented here provide quantitative analysis of key components of this work (including type I peripheral fibre cross-sectional area and fibre density, and SGN density and soma area). Some findings are presented as qualitative observations; in all these cases, we have carefully chosen images that provide clear representation of the ultrastructural features we observed during TEM analysis.

Deafness-Induced Changes in the Organ of Corti

The effects of duration of deafness on the terminal nerve endings and the degeneration of the organ of Corti were examined in transverse sections (Fig. 3). In the untreated control organ of Corti, IHCs and supporting cells had a normal appearance (Fig. 3a, e). Afferent nerve terminals innervated the IHCs and efferent nerve terminals made connections with these afferent endings. Following deafening, click-evoked ABRs were absent (i.e. thresholds greater than 100 dB p.e. SPL; data not shown). Two weeks following deafening the organ of Corti had degenerated with the complete loss of IHCs (Fig. 3b) and OHCs (data not shown) in the basal turn. However, around the region of the missing IHCs, numerous afferent and efferent nerve endings were evident in between the residual supporting cells (Fig. 3f). Following a period of 6 weeks of deafness, the basic structure of the organ of Corti was still recognisable (Fig. 3c) with some residual supporting cells present and some structural elements identifiable (such as the tunnel of Corti). However, the number of remaining nerve endings at locations corresponding to the place of the missing IHCs had decreased (Fig. 3g). At 12 weeks following deafening, the supporting cells were no longer present and only a monolayer of squamous cells remained on the basilar membrane (Fig. 3d). Very few neurite profiles were evident (Fig. 3h).

Deafness-Induced Changes in Type I SGN Peripheral Fibres

The effect of deafening on peripheral fibres was examined by measuring their cross-sectional area at both the distal and medial OSL sites (Fig. 1c). Examples of peripheral fibre cross sections in a normal hearing cochlea are shown in Fig. 4a, e. Examination of the peripheral fibre cross sections from deafened animals at low magnification showed several notable features. With increasing durations of deafness, there was a reduction in the density of myelinated fibres within the OSL compared with the normal control. The most dramatic reduction was observed following 6 weeks of deafness (Fig. 4c, g). Often, the myelin profiles were completely, or nearly completely, devoid of axoplasm, indicating that the peripheral fibres had retracted within the myelin sheath before the sheath was subsequently broken down and cleared.

The cross-sectional area of the peripheral fibres was examined in OSL sections and a one way ANOVA on ranks was performed. There was no effect of cochlear region (region 1: lower basal versus region 2: upper basal; Fig. 1b) but there was a significant effect of OSL position whereby fibres measured in the distal

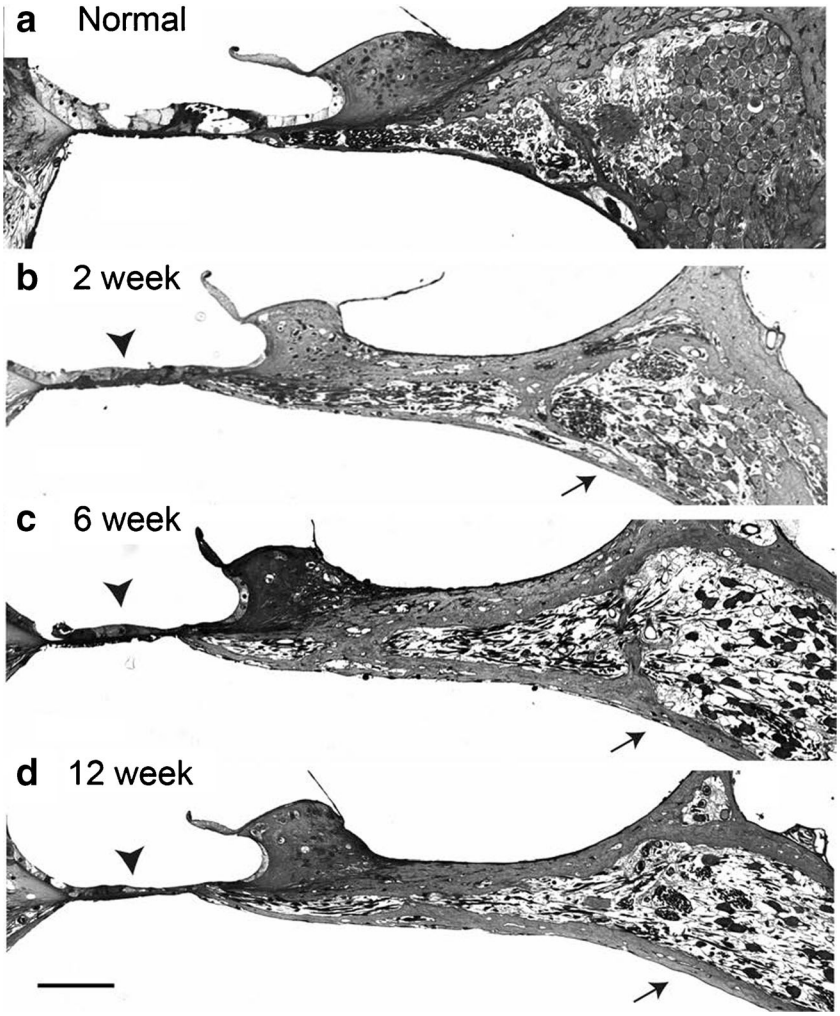

FIG. 2. Representative light microscope images illustrating the deafness-induced changes in the basal turn from each cohort in the present study. **a** Normal hearing cochlea. **b** 2-week deafened. **c** 6-week deafened. **d** 12-week deafened. *Scale bar* = 100 μm. *Arrowheads* indicate the flattened sensory epithelium and *arrows* indicate the Rosenthal's canal with reduced SGN density.

OSL were significantly smaller than fibres measured in the medial OSL ($p < 0.02$) in the normal cochleae. Therefore, non-parametric statistical analysis was carried out on the medial and the distal OSL positions individually using a one way ANOVA on ranks, based on measurements from 1035 myelinated fibres (normal cochlea = 221, 2-week deaf = 331, 6-week = 269, and 12-week = 214). There was a significant effect of deafness duration for both the medial and distal positions ($p < 0.001$) indicating that fibre area became significantly smaller over time with most of the changes occurring within the first 2 weeks of deafness (Fig. 5a).

Analysis of the density of peripheral fibres across the normal and deafened cohorts was also performed and shown to be normally distributed. These data were based on measurements from 1783 myelinated fibres across medial and distal OSL locations (normal cochlea = 555, 2-week deaf = 652, 6-week = 257, and 12-week = 319). There was no difference in fibre density for different cochlear regions (region 1 versus region 2) in normal control cochleae, and no difference in location (distal versus medial) (three-way ANOVA) and data was therefore collapsed (Fig. 5b). There was a significant main effect of the duration of deafness (three-way ANOVA $p < 0.001$). Post hoc analysis indicated a significant decrease in the density of fibres in the normal and 2-week deafened cochleae compared to 6-week and 12-week deafened cochleae (Holm–Sidak $p < 0.001$, differences indicated in Fig. 5b). Similarly, there was a significant increase in the density of degenerating fibres in the deafened animals with the post hoc analysis indicating significantly lower density of degenerating fibres in the normal compared to all the deafness durations (Holm–Sidak Method, $p < 0.05$). Although there was a trend for the density of degenerating fibres to decrease with increasing duration of deafness, the overall proportion of degenerating-to-normal fibres was greater at the

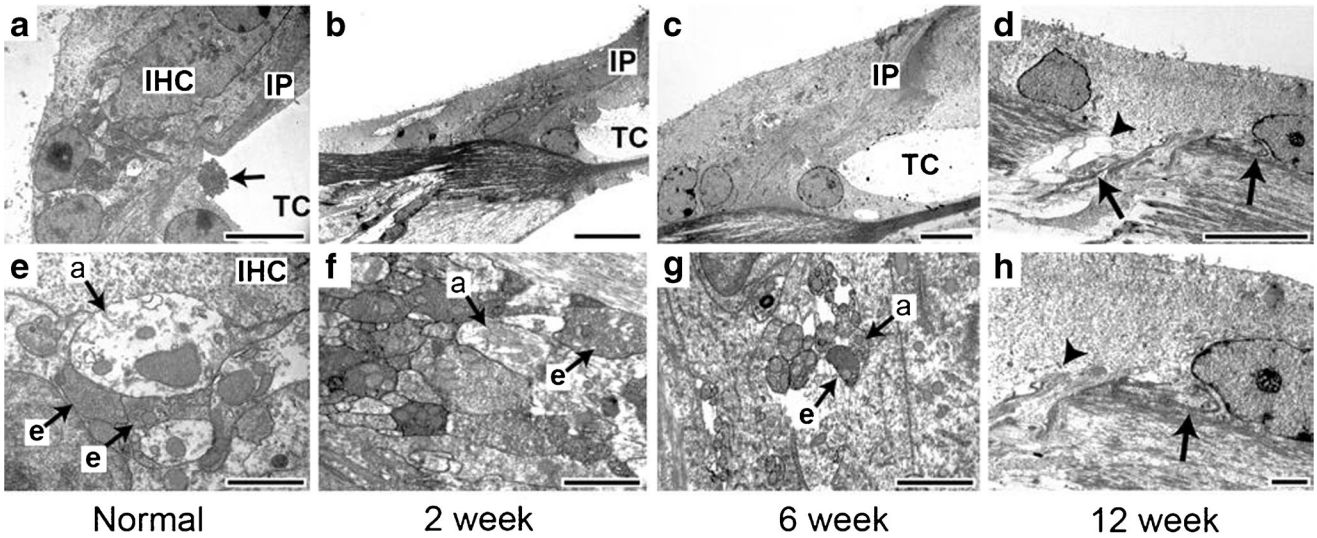

FIG. 3. The effect of duration of deafness on terminal nerve endings in the organ of Corti for region 1 (see Fig. 1). Low (*top panel*) and high magnification (*bottom panel*) images taken at the location of the inner hair cell (*IHC*) near the habenula perforata. **a**, **e** Images from a normal hearing cochlea showing terminal nerve endings, an IHC, and supporting cells (*IP*—inner pillar cell, *TC*—tunnel of Corti, *arrow* points to the tunnel spiral bundle). At high magnification (**e**), the basal portion of an IHC is contacted by an afferent fibre (*a*), which is in turn contacted by two efferent (*e*) vesiculated endings. **b**, **f** Images from a 2-week deafened cochlea. The IHC has degenerated but an inner pillar cell (IP) is still clearly visible. **f** Numerous nerve endings, both afferent (*a*) and efferent (*e*), were present within the residual structures of the organ of Corti. **c**, **g** Images from a 6-week deafened cochlea. The inner pillar cells (IP) were still clearly visible and the organ of Corti had some structural integrity as indicated by the presence of the tunnel of Corti (TC), which had begun to collapse. **g** The higher magnification image shows few remaining small afferent and efferent nerve endings (*arrow a* and *e*). **d**, **h** Images from a 12-week deafened cochlea. A monolayer of cells appeared at the place of the degenerated organ of Corti. At the habenula perforata (*arrowhead*), a small number of nerve profiles were still visible extending in between the basilar membrane and the monolayer epithelium (*arrow*). *Scale bars* (**a**–**d** = 5 μm, **e**–**h** = 1 μm).

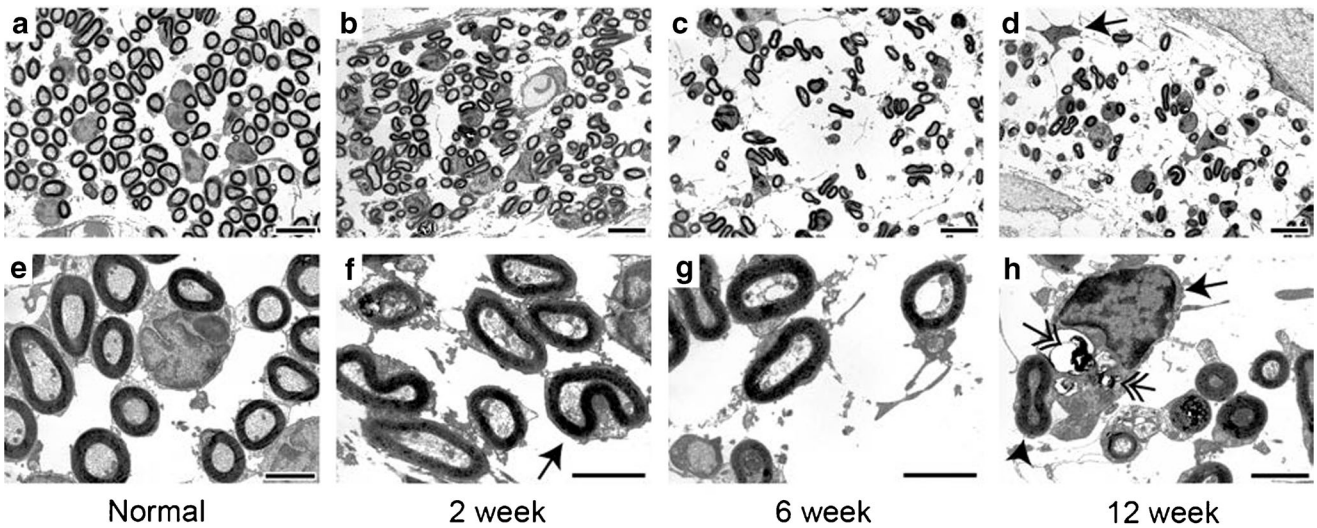

FIG. 4. The effect of deafening on peripheral fibres. Representative images of peripheral fibres within the OSL (medial OSL sections), at low (*top panel* **a**–**d**) and higher (*bottom panel* **e**–**h**) magnification. **a**, **e** In the normal hearing cochlea, regularly shaped and densely packed fibres, together with some Schwann cells, were evident. **b**, **f** After 2 weeks of deafening, the overall density of myelin profiles had not changed; however, at high magnification (**f**), more irregular shaped myelin profiles (*arrow*), reduction in fibre area, and evidence of early stage of axoplasm retraction were observed. **c**, **g** Following 6 weeks of deafness, the density of fibres had decreased dramatically. Many remaining myelin profiles exhibit retraction of the axoplasm, but the remaining myelin sheaths were well preserved. **d**, **h** After 12 weeks of deafness, the density of fibres was further reduced. An example of a Schwann cell (**d**: *arrow*) that appeared to have lost connection with its peripheral fibres appeared to have dedifferentiated into a non-myelinating phenotype. **h** A Schwann cell (*large arrow*) not only provided myelin to a fibre with normal morphology (*arrowhead*) but also ensheathed remnants of two other degenerated fibres (*double arrows*). *Scale bars* (**a**–**d** = 5 μm, **e**–**h** = 2 μm).

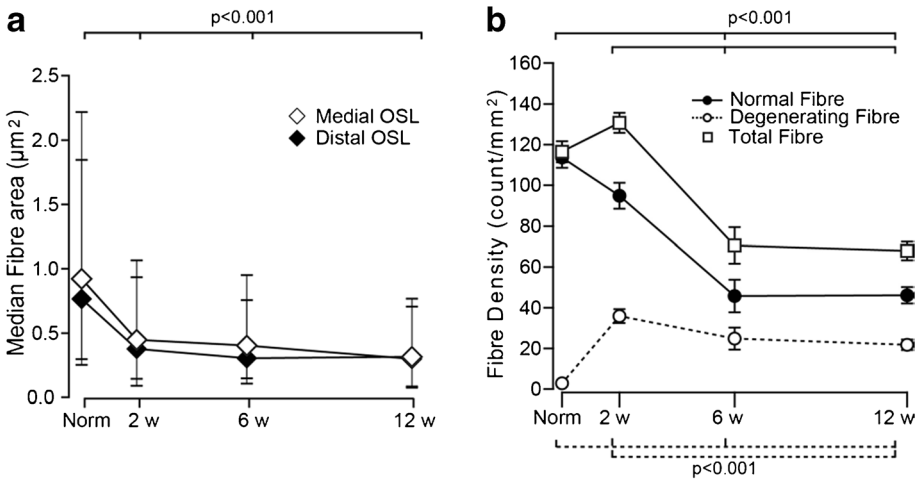

FIG. 5. Morphological changes in peripheral fibres with duration of deafness. **a** Median fibre area for normal (*Norm*) cochleae and following 2 (*2w*), 6 (*6w*), and 12 (*12w*) weeks of deafness measured at the medial and distal position within the OSL. There was a significant reduction in fibre area following the onset of deafness (main effect, ANOVA, $p < 0.001$) that stabilised after 6 weeks. The median, 25th, and 75th percentiles are illustrated. **b** Analysis of the distribution of fibres undergoing degeneration from anatomically normal fibres. The mean density of anatomically normal fibres (*solid lines*) decreased with duration of deafness (as indicated by the *significance bars*). The density of degenerating fibres (*dashed lines*) increased significantly 2 weeks following deafness and then plateaued. Total fibre density is indicated by *open squares*. Note that the total 2-week fibre density count is greater than the normal controls. This is likely to be a result of a slight bias as a result of the significant reduction in fibre area at 2 weeks. *Error bars* = SEM.

longer deafness time points (38 % 2 weeks compared to 54 % at 6 weeks and 47 % at 12 weeks).

The type I SGN peripheral fibres were also examined in longitudinal cross sections within the OSL (see Fig. 1). The peripheral fibres were myelinated by Schwann cells within the OSL. In both normal and deafened cochleae, we frequently observed individual Schwann cells that appeared to provide myelin to more than one peripheral fibre (Fig. 6a–f). A number of Schwann cells in the OSL of the 6- and 12-week deafened cohorts appeared to undergo dedifferentiation into a non-myelinating phenotype following loss of contact with their peripheral fibres (Fig. 6g–i).

Examples of peripheral fibres at low and high magnification in a normal and a 6-week deafened cochlea are illustrated in Figure 7. A key feature of peripheral fibre degeneration was the retraction of the fibre's axoplasm leaving an apparently normal myelin sheath (Fig. 7b, d). Although sometimes myelin degeneration or delamination was observed, it did not usually occur in concert with the retraction of the axoplasm, suggesting two independent mechanisms of degeneration. An example of this sequence of degeneration is shown in Figure 7b, d. There is no apparent difference between the myelin sheath in a peripheral fibre undergoing degeneration compared to that observed in a normal cochlea (compare Fig. 7c, d). Large unmyelinated fibres that exhibited morphological features similar to type I SGN peripheral fibres were occasionally observed in the OSL of deafened cochleae (Fig. 7e, f). There was no evidence of myelin breakdown products, such as myelin figures, suggesting that these fibres were not undergoing demyelination. It is possible that these fibres were resprouting neurites that had yet to be myelinated.

Deafness-Induced Changes in Type I Spiral Ganglion Neurons Within Rosenthal's Canal

Type I SGNs within Rosenthal's canal were examined in transverse sections from the basal turn (Fig. 1c). Figure 8 shows examples of type I SGN soma from a normal, 2-, 6-, and 12-week deaf cochleae at low (top panel) and higher (bottom panel) magnification.

The cytoplasmic contents exhibited by normal type I SGNs included densely packed polyribosomes, numerous mitochondria, lipid granules, and Golgi apparatus. There was little difference in the packing density, soma area, and ultrastructure of type I SGN soma 2 weeks following deafening (Fig. 8b, f) compared to the normal cochleae (Fig. 8a, e). Following longer periods of deafness, there was a significant decrease in type I SGN density (Fig. 8i; ANOVA, $p < 0.001$) that was progressive over time, and a significant reduction in soma area (Fig. 8j; ANOVA, $p < 0.003$) that stabilised after 6 weeks of deafening (i.e. no significant change in soma area between 6 and 12 weeks of deafness). The intracellular content of the majority of remaining type I SGN soma appeared similar to normal cochleae (e.g. compare Fig. 8e with Fig. 7h). Occasionally, large intercellular vacuoles were observed among the profiles of type I SGNs, but this was observed in both normal and deafened cochleae. Remnant basement

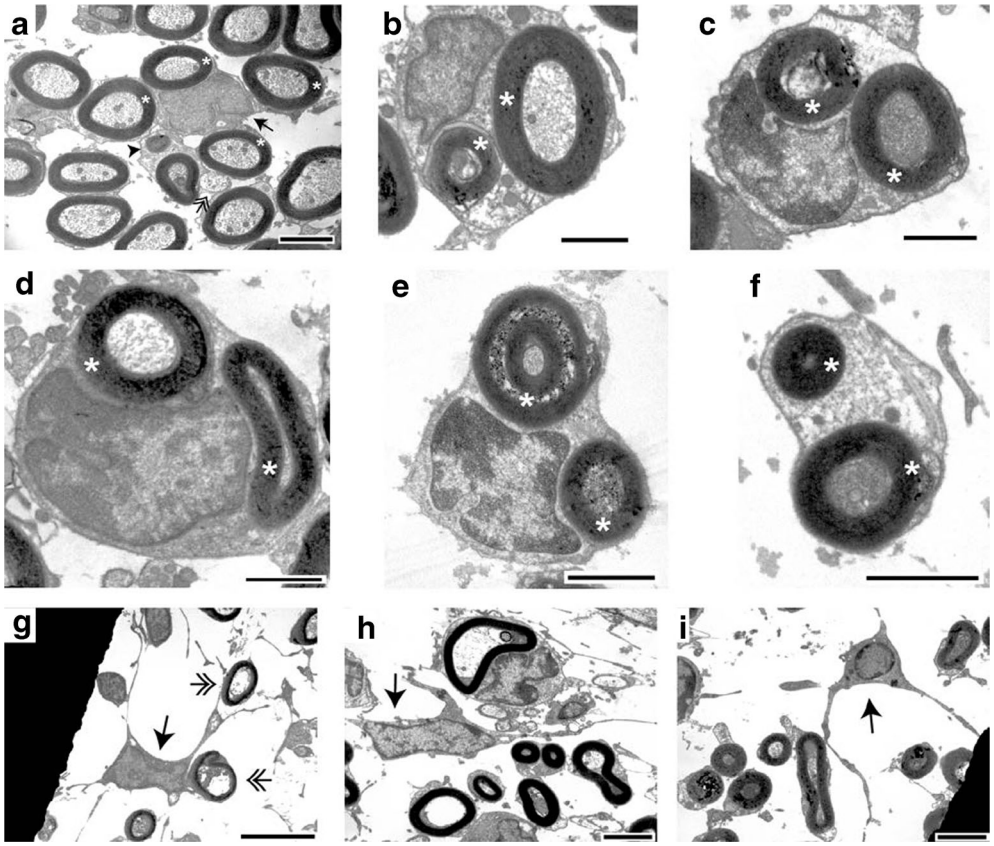

FIG. 6. Peripheral fibres within the OSL. **a** OSL cross sections from a normal hearing cochlea. Schwann cells (*arrow* and *arrowhead*) appear to be providing myelin for a number of peripheral fibres (*white stars*) that were wrapped by small cytoplasmic processes. A Schwann cell (*arrowhead*) ensheaths both a myelinated fibre and an unmyelinated fibre (*double arrow*). **b**, **c** Higher magnification images from a normal cochlea showing examples of two peripheral fibres (*asterisk*) that were ensheathed by one Schwann cell. **d**–**f** Examples of two peripheral fibres (*asterisk*) that were ensheathed by a single Schwann cell in deafened cochleae. **g**–**i** Examples of Schwann cells (*arrow*) that appeared to have dedifferentiated in response to the loss of their peripheral fibres. Two fibres (**g**: *double arrows*) have undergone significant degeneration and were almost completely devoid of axoplasm. *Scale bars* (**a** = 2 μm, **b**–**f** = 1 μm, **g** = 5 μm, **h** and **i** = 2 μm).

membranes, most likely from surrounding Schwann cells or degenerated type I SGN soma, were often observed after 6 and 12 weeks of deafness.

Only small numbers of type I SGN soma were observed undergoing degeneration at each time point following deafening suggesting a rapid degeneration process. The degeneration first affected the type I SGN soma followed later by its satellite Schwann cell. Two forms of degeneration were observed among SGNs: (i) an apoptotic-like compaction of the nucleus and cytoplasm (Fig. 9a, b) or (ii) a necrotic-/cytolytic-like degeneration (Fig. 9c, d). Following degeneration of the SGN, the myelin (which once ensheathed the type I SGN soma) disappeared, leaving only a non-myelinating Schwann cell for a period of time as the only indicator of the former presence of the type I SGN (Fig. 9d).

Although the intracellular content of the majority of remaining type I SGNs in the deafened cochlea appeared normal (e.g. Fig. 8f–h and Fig. 9a), some type I SGNs exhibited an ectopic morphology with sprout-like protrusions of the cytoplasm (Fig. 10). These protrusions were covered by a normal myelin sheath and tended to occur at or close to the soma (Fig. 10a, b), or the axon hillock (Fig. 10c).

Deafness-Induced Changes in Schwann Cells Within Rosenthal's Canal

Although satellite Schwann cells exhibited greater survival traits than SGNs, their morphology changed following the loss of the type I SGN soma. Schwann cells appeared to dedifferentiate into a non-myelinating phenotype in a manner similar to that observed in the OSL following the retraction of the peripheral fibre. This dedifferentiation was accompanied by the formation of glial processes that extended into the surrounding environment (Fig. 11). The Schwann cell soma assumed an 'astrocyte-like' morphology as these processes extended seemingly in an attempt to interact with residual type I SGNs. This change is highlighted by the difference in the morphology of the two Schwann cells shown in Figure 11a. One Schwann cell (arrowhead)

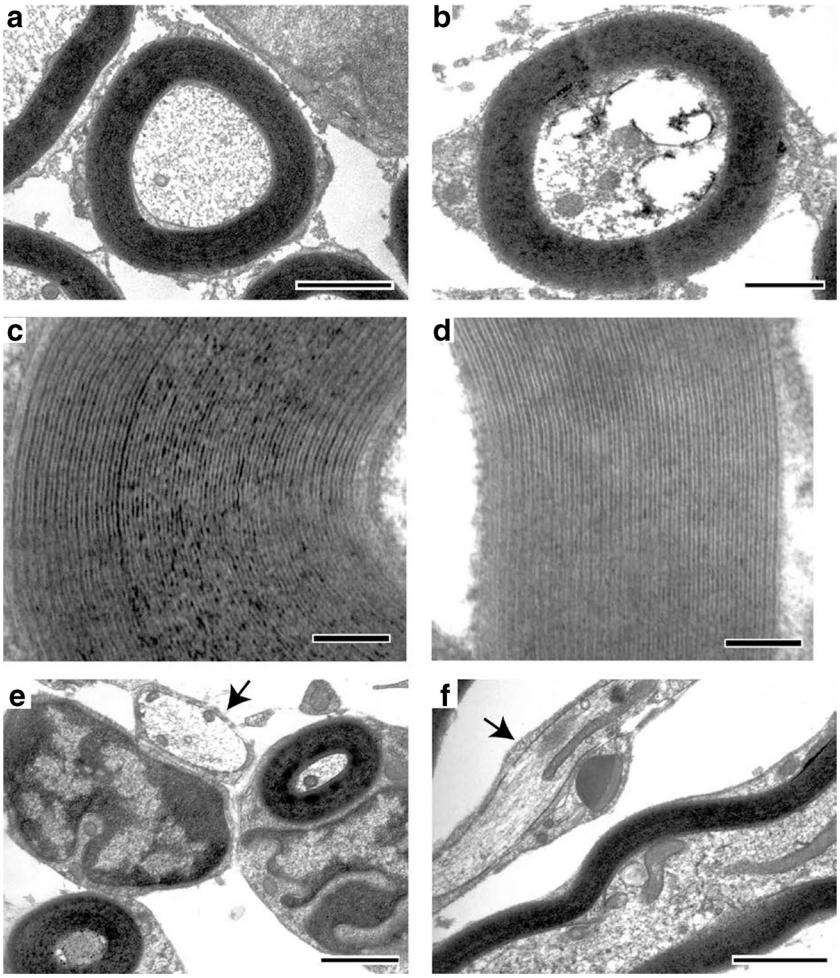

FIG. 7. Myelin sheath of a normal and degenerating peripheral fibre. **a**, **c** A peripheral fibre in a normal cochlea with an intact myelin sheath. **b**, **d** A peripheral fibre in a 6-week deafened cochlea that had begun to degenerate as evidenced by the collapse and retraction of the fibre's axoplasm. The myelin sheath surrounding the degenerating fibre appeared normal. **e**, **f** Examples of large unmyelinated fibres (*arrow*) from a 6-week deafened cochlea in a cross section (**e**) and a longitudinal section (**f**) of the OSL. Schwann cells ensheathed but did not myelinate these fibres. The morphological features of these fibres (relatively large size, neurofilament, and microtubule content) are consistent with neighbouring type I SGN peripheral fibres. *Scale bars* (**a** = 1 μm, **b** = 0.5 μm, **c** and **d** = 0.1 μm, **e** and **f** = 1 μm).

remained connected to a surviving type I SGN while the second (arrow) had lost its SGN (*) and assumed an astrocyte morphology. Additional examples are shown in Figure 11b, c illustrating the extension of glial processes from the Schwann cell soma. Figure 11d–f shows a Schwann cell process attempting to make contact with two surviving type I SGNs that already had a Schwann cell and an intact myelin sheath. The process from the dedifferentiated Schwann cell appeared to interact with these type I SGNs, altering the morphology of the SGN soma.

DISCUSSION

This study described the degenerative changes in type I SGNs and their Schwann cells in the basal turn of the guinea pig cochlea following an aminoglycoside-induced sensorineural hearing loss. These changes were initially characterised by complete loss of hair cells within the first 2 weeks following deafening, the relatively rapid loss of unmyelinated axons within the organ of Corti, and the shrinkage and retraction of the axoplasm of peripheral fibres within the OSL. Changes to the peripheral nerve fibres were statistically significant as early as 2 weeks post deafening. Although the myelin sheath initially remained intact, it subsequently collapsed and was rapidly cleared. Significant reductions in both SGN soma area and density within Rosenthal's canal became evident after 6 weeks of deafness. Ongoing degeneration of SGNs was observed such that SGN density was 35 % of normal levels after 12 weeks of deafness. Despite

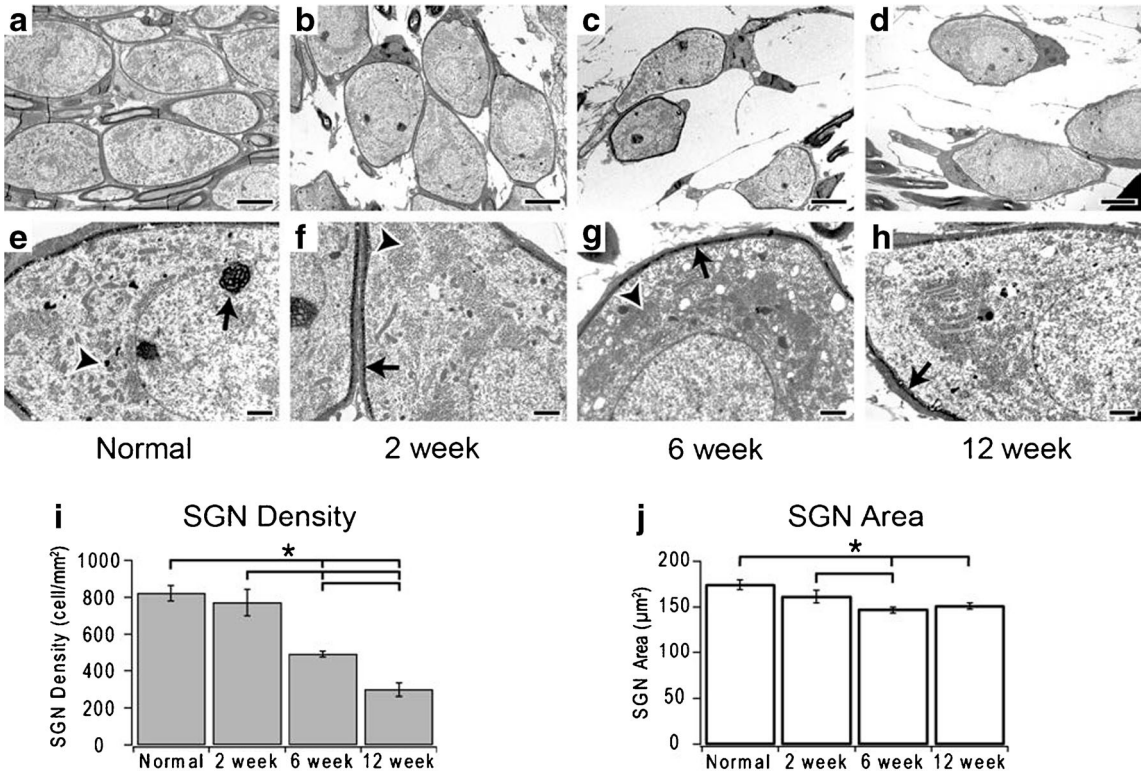

FIG. 8. Effect of deafness duration on type I SGN cell bodies. Representative images of SGN soma at low (*top panel*) and higher (*bottom panel*) magnification. **a**, **e** Examples from a normal hearing cochlea. **a** The soma of the type I SGNs were typically oval shaped, myelinated, and densely packed. The higher magnification image (**e**) shows the classical ultrastructure of a type I SGN cell body, covered by a few layers of myelin sheath, densely packed polyribosomes, numerous mitochondria, and lipidic granules (*arrowhead*). Nucleoli (*arrow*) are clearly visible in the cell nucleus. **b**, **f** Examples from a 2-week deafened cochlea. Very few, if any, changes in cellular ultrastructure were observed. A normal myelin layer (*arrow*) and polyribosomes (*arrowhead*) were evident. **c**, **g** Examples from a 6-week deaf cochlea. The cell density (quantified data in **i**) and soma area (quantified data in **j**) had decreased significantly. However, most of the remaining type I SGNs, although smaller, appeared to have a normal myelin sheath (*arrow*) and intracellular content (**g**; *arrowhead*). **d**, **h** Examples from a 12-week deafened cochlea. A progressive loss of type I SGNs was observed (65 % reduction by 12 weeks). However, again, the intracellular contents of most of the remaining type I SGNs appeared to be consistent with a normal cochlea including intact myelin (*arrow*). The graphs indicate type I SGN density (**i**) and soma area (**j**) plotted against duration of deafness. There was an ongoing decrease in type I SGN density (*ANOVA, $p < 0.001$) in addition to a decrease in soma area (*ANOVA, $p < 0.003$) that had stabilised by 12 weeks of deafness. *Error bars* represent standard error of the mean (*SEM*). *Scale bars* (**a**–**d** = 5 μm, **e**–**h** = 1 μm).

evidence of shrinkage, residual type I SGN soma in deafened cochleae exhibited similar intracellular content to type I SGNs from normal cochleae although they occasionally exhibited an altered morphology following contact with dedifferentiated Schwann cells or the formation of ectopic neurites. Only a small number of SGNs were observed undergoing degeneration, which occurred either via apoptotic or necrotic mechanism, suggesting that once initiated, the degeneration of the SGN soma was rapid. Finally, following loss of the type I SGN, the residual satellite Schwann cell, devoid of neural contact, dedifferentiated into a non-myelinating phenotype and formed processes that appeared to be attempting to make contact with residual SGNs. A schematic representation of these key observations is depicted in Figure 12.

Deafness-Induced Changes in the Organ of Corti

The effects of aminoglycoside exposure has been characterised previously with regard to hair cells (Forge 1985; Ladrech et al. 2007) and their SGN synapses (Terayama et al. 1979; Lenoir et al. 1999). The degenerative effects of deafness are most prevalent in the basal region of the cochlea (Leake and Hradek 1988; Zimmermann et al. 1995; Hardie and Shepherd 1999) and therefore, our study focused on this region. In the present study, all hair cells in the basal turn degenerated within the first 2 weeks following deafening, leaving behind residual columnar cells that were eventually replaced by a single layer of squamous cells on the basilar membrane—the so-called flattened epithelium (Ladrech et al. 2007; Raphael el al. 2007) Although the terminals of type I afferent fibres remained localised to the region of the

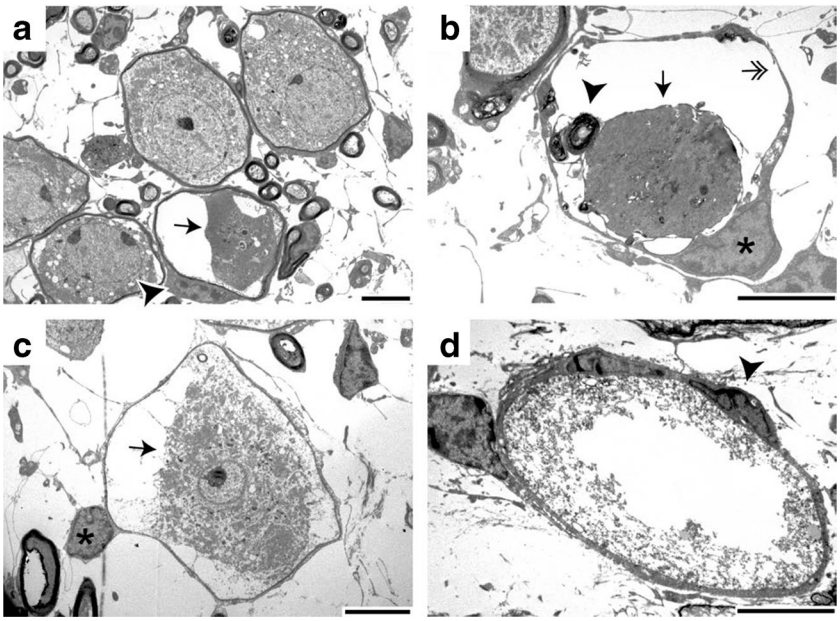

FIG. 9. Degeneration processes of type I SGNs following 6 weeks of deafness. **a** A type I SGN (*arrow*) in the process of degeneration via apoptosis. However, the Schwann cell (*arrowhead*) and its myelin sheath surrounding the neuron appeared normal. **b** Example of a type I SGN in a more advanced stage of apoptotic degeneration (*arrow*). The Schwann cell exhibited a normal soma (*asterisk*) and formed a 'bed' around the degenerating neuron. However, demyelination was also evident (*double arrow*) and some myelin remnants (*arrowhead*) can be seen. **c** Example of a type I SGN undergoing degeneration via a cytolytic process. The soma of the Schwann cell is indicated by *asterisk*. **d** Example of a more advanced cytolysis of a type I SGN still ensheathed by its satellite Schwann cell (*arrowhead*). *Scale bars* = 5 μm.

lost IHCs over the first few weeks following deafening, by 12 weeks, only sporadic nerve fibres were observed between the basilar membrane and the flattened epithelium.

Deafness-Induced Changes to Type I SGN Peripheral Fibres Within the OSL

The degeneration of type I SGN peripheral fibres demonstrated a significant reduction in the cross-sectional area of peripheral fibres as early as 2 weeks following deafness, with the fibres in the distal region of the OSL exhibiting a more extensive reduction in axoplasm.

In concert with axonal shrinkage, there was a significant decrease in peripheral fibre density. The axoplasm of peripheral fibres retracted, leaving behind an apparently normal myelin sheath even when completely devoid of axoplasm, a finding consistent with that reported by Waaijer et al. (2013). This was a common observation in the present study and suggests that extensive demyelination of residual peripheral fibres is not a primary feature of deafness-associated degeneration of type I SGNs in the ototoxic

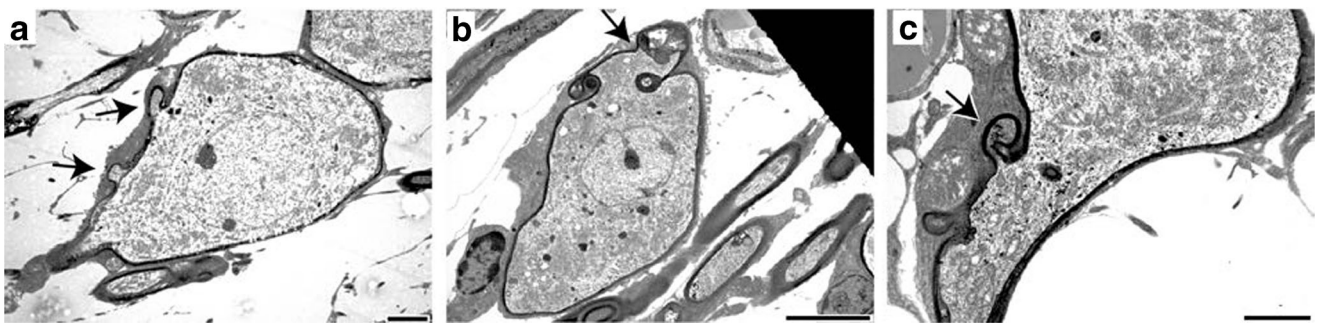

FIG. 10. Ectopic morphology of type I SGNs in 6-week deafened cochleae. Deafened cochleae contained type I SGNs that exhibited an altered morphology. In some cases, this was associated with neuronal sprouting. Although the cytoplasmic structure and myelin of these neurons appeared anatomically normal, the morphology varied substantially from the oval shape type I SGN observed in normal cochleae (e.g. Fig. 8a). Neural sprouting arising from the SGN soma (*arrow*; **a** and **b**) or the axon hillock (*arrow*; **c**) was observed in some SGNs of deafened cochleae. All examples in this figure were taken from 6-week deafened cochleae although similar features were observed in the 12-week deafened cohort. *Scale bars* (**a** = 5 μm, **b** and **c** = 2 μm).

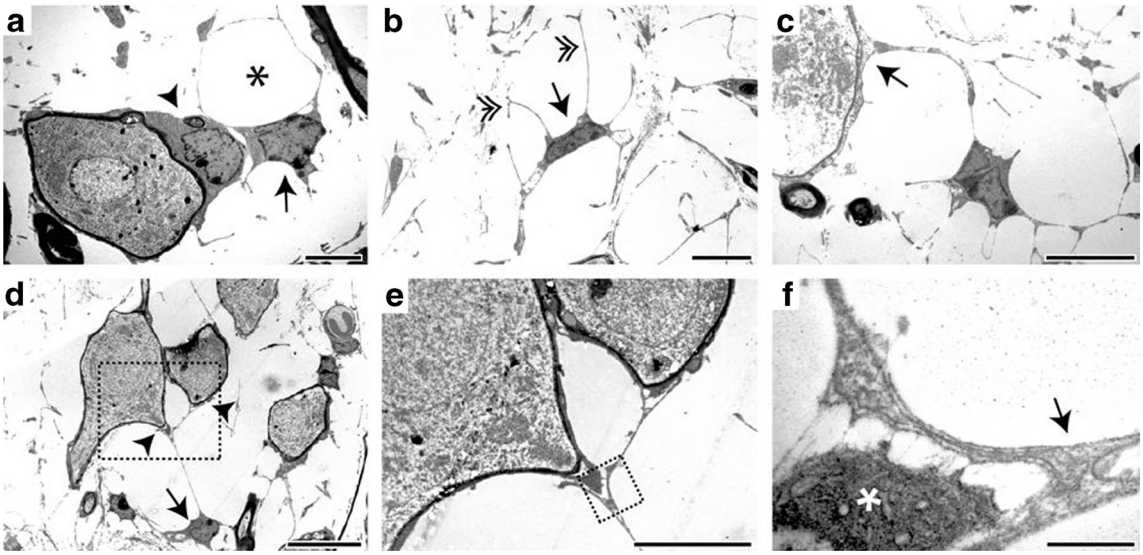

FIG. 11. Schwann cell dedifferentiation. Images from a 6-week deafened cochlea. **a** An example of a Schwann cell (*arrow*) that had lost its SGN (*asterisk*) and had begun to dedifferentiate into a non-myelinating phenotype. Nearby is a type I SGN with normal morphology, myelinated by its Schwann cell (*arrowhead*). **b** An example of a Schwann cell (*arrow*) dedifferentiating after the loss of the SGN. This Schwann cell had an astrocyte-like profile, with long processes (*double arrows*) extending from the soma. **c** Another dedifferentiated Schwann cell extended processes from its soma and contacted the glial sheath of a surviving SGN (*arrow*). **d** A dedifferentiated Schwann cell (*arrow*) contacted new targets (*arrowheads*). An elongated process contacted two neurons already ensheathed (and myelinated) by their own Schwann cells. The region within the *framed box* is represented in higher magnification in **e** showing that the process appeared to alter the morphology of the contacted SGNs. **f** Higher magnification (framed in **e**) of this contact region showing more clear filaments between the dedifferentiated glial process membrane (*arrow*) and the glial sheath (*asterisk*) of one of the two neighbouring SGNs. *Scale bars* (**a**–**c** = 5 μm, **d** = 10 μm, **e** = 5 μm, **f** = 0.5 μm).

deafness model. Finally, after a period of time, the myelin sheath collapsed and was rapidly cleared.

In both normal and deafened cochleae, we occasionally observed examples where two or more fibres appeared to be supported and myelinated by one Schwann cell in a manner more reminiscent of oligodendrocytes in the central nervous system (e.g. Fig. 6). Although reported earlier in the cat (Adamo and Daigneault 1973), this feature has received little attention in the literature, presumably due to limited TEM analysis of the OSL.

Finally, our analysis did not distinguish myelinated afferent and efferent fibres in the OSL. The medial efferents are known to have a very specific course from Rosenthal's canal (where they form the intraganglionic spiral bundle (IGSB)) to the organ of Corti (Brown 1987a). While the efferent bundle leaving the IGSB cannot be sectioned in the same orientation as the type I afferents, it is possible to confuse the fibre types when examining radial fibres within the OSL as both fibre types are myelinated, both cross the OSL in a radial direction, and the medial efferents in the guinea pig OSL are only slightly smaller than the type I afferents (up to 1.2 μm diameter versus 1.7 μm, respectively) (Brown 1987b, a). Although the identification of type I afferents versus medial efferents in the OSL present some difficulties, it is important to note that the number of medial efferent fibres is significantly less than the type I afferent comprising approximately 25 % of the population of myelinate fibres (Morrison et al. 1975). Moreover, medial efferent fibres undergo far more rapid degeneration compared with the type I afferent following hair cell loss (McFadden et al. 2004). Therefore, while the identification of fibre type presents some challenges, the large difference in population and the rapid degeneration of the efferents reduce the significance of this issue.

Peripheral Fibre Morphology

In deafened cochleae, we occasionally observed large unmyelinated fibres that had morphological characteristics of type I SGN peripheral fibres (axoplasm composition and size) that differentiated them from the smaller, unmyelinated type II SGN fibres and lateral efferents. We consider these fibres were recently regenerated type I SGN peripheral fibres. It is known that SGNs in deafened cochleae have an inherent capacity to regenerate their peripheral fibres (Bohne and Harding 1992) and that the exogenous application of growth factors can enhance this regeneration (Wise et al. 2005; Glueckert et al. 2008; Leake et al. 2011). Although not examined here, previous studies of deafened cochleae have shown that resprouting fibres can exit the habenula perforata and course within the cellular layer of the inner

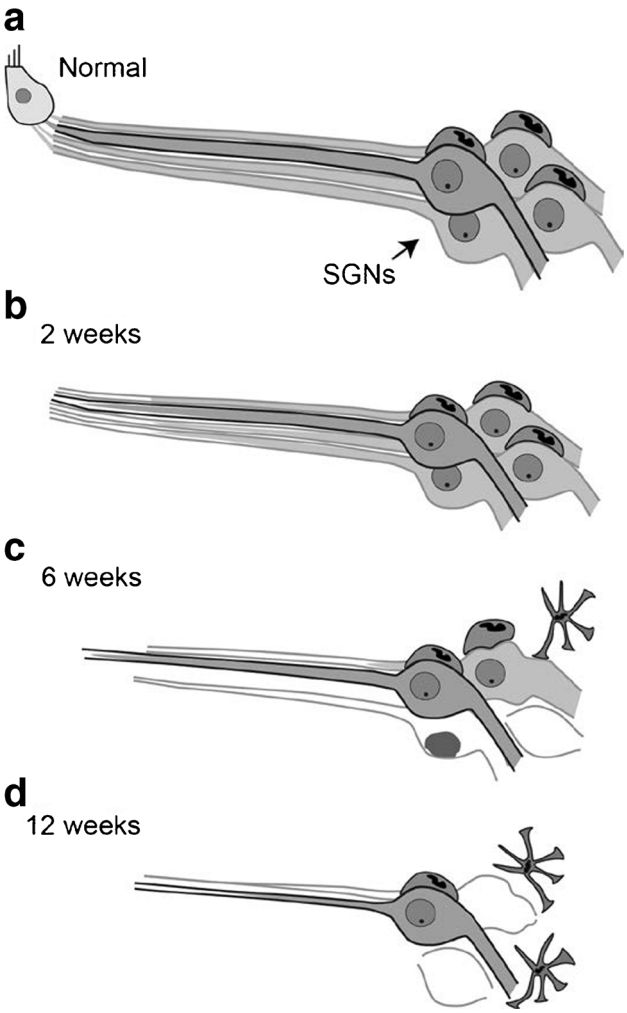

FIG. 12. Schematic representation of the key features of type I SGN degeneration and the dedifferentiation of myelinating Schwann cells in the transverse orientation. **a** In the normal cochlea, a number of peripheral fibres make synaptic connections with an inner hair cell. There is a full complement of SGNs with their soma in Rosenthal's canal. Schwann cells are associated with both types of SGNs but only myelinate type I SGNs. **b** Two weeks following hair cell loss, the axoplasm within the peripheral fibres begins to shrink and retract towards the soma while the myelin sheath remains intact. There is no SGN loss at this stage. **c** After 6 weeks of deafness, retraction of the peripheral fibres is more extensive, and ~50 % of the type I SGNs have degenerated via apoptotic or necrotic mechanisms. The myelin sheath associated with early degenerated SGNs has also collapsed. Schwann cells lose connection with the degenerated SGNs and dedifferentiate temporally leaving behind a glial bed and sending out processes to sample the local environment. Residual type I SGNs exhibit altered morphology. **d** After 12 weeks of deafness, about two thirds of the SGNs have degenerated. Greater numbers of Schwann cells undergo dedifferentiation into a non-myelinating phenotype.

sulcus, loop within the OSL, or project into the scala tympani—locations in which SGN fibres are not normally observed (Spoendlin and Suter 1976; Strominger et al. 1995; Bohne et al. 1999; Richardson et al. 2005; Landry et al. 2013).

Deafness-Induced Changes to the Type I SGN Soma

The progressive shrinkage and loss of type I SGNs with increasing duration of deafness described in the present study are well characterised in animal models of deafness (Leake and Hradek 1988; Leake et al. 1999; Lenoir et al. 1999; Forge and Schacht 2000; McGuinness and Shepherd 2005) as well as human material (Nadol et al. 1989). Our findings showed a significant decline in SGN density with increasing duration of deafness such that there was a reduction in cell density of 65 % after 12 weeks. In addition, there was significant shrinkage of the SGN cell bodies to approximately 85 % of normal, although this had stabilised by the 6-week period.

There were a number of important features observed in type I SGN of deafened ears evident in the present study. First, the cytoplasmic content at the ultrastructural level appeared similar to SGNs within normal cochleae, even following 12 weeks of deafness. This finding supports previous TEM studies (Spoendlin 1975; Ylikoski et al. 1975) and implies that long-term deafened SGNs maintain the cytoplasmic machinery required to generate and propagate action potentials in response to electrical stimulation (Shepherd and Javel 1997).

Second, although the surviving type I SGN soma in deafened ears appeared relatively normal, we did observe some morphological abnormalities. These changes occurred when the process of a dedifferentiated Schwann cell made contact with the SGN (see "Discussion" below). Although not commonly observed, neurites were evident sprouting from the soma of some type I SGNs in deafened cochleae. The long-term fate of these putative resprouting fibres remains to be determined. It is likely that if they cannot make synaptic connections, or obtain trophic support from other cells, they will eventually atrophy and degenerate (Terayama et al. 1979).

Third, the residual type I SGNs in the deafened cochleae were often situated in close proximity to remnants of degenerated SGNs and would have projected to the same region of the organ of Corti, indicating that the local cochlear environment was not a key factor in determining which SGNs degenerated. It would appear that type I SGNs are not equally susceptible to degeneration following loss of the inner hair cell. There is evidence that SGNs with high acoustic thresholds (low spontaneous rates) are more susceptible to noise trauma and may preferentially degenerate (Kujawa and Liberman 2009). However, it remains to be determined why one SGN degenerates while neighbouring neurons appear ultrastructurally normal (if somewhat smaller in size) for long periods of time following loss of their sensory epithelium. A genetically distinct sub-population of type I SGNs may be resilient to sensorineural hearing loss.

Fourth, type I SGNs appeared to undergo degeneration via one of two mechanisms following loss of the inner hair cell: (1) an apoptotic mechanism whereby the cytoplasmic content of the shrunken SGNs became dense and tightly packed with condensation of the chromatin and discontinuities in the cell membrane and (2) a cytolytic, also described elsewhere as an autophagic (Menardo et al. 2012) or necrotic mechanism, whereby the cytoplasm and the nucleus became loosely fragmented and deteriorated (Dodson 1997). The infrequent observations of SGNs undergoing degeneration in the present study suggested that both degeneration pathways were rapid. These observations are consistent with previous results in the rat showing that the expression of Caspase 3 (a cell death marker) was only observed in 1–2 % of cells examined and that the apoptotic process was completed within a few hours (Ladrech et al. 2004).

Finally, we note that given the 15 % reduction in SGN soma area observed over the course of the study, we cannot dismiss the possibility of over-counting SGNs. While a correction factor to account for this shrinkage was not used here, we mitigated against any bias by only including SGNs with a clear nucleolus and separating sections by at least 24 µm to ensure that each SGN is only counted once.

Type I SGN Degeneration Following Aminoglycoside Toxicity Is Secondary to Hair Cell Loss Rather than a Direct Insult on SGNs

The results of the present study support the observation that the pathological changes to type I SGNs were secondary to the loss of hair cells, although we cannot conclusively rule out that the normal pathology observed was a result of direct SGN insult. We showed that the longitudinal degeneration of type I SGN peripheral fibres occurred following the rapid and complete loss of hair cells and the collapse of the organ of Corti in the basal turn. Large numbers of type I SGN peripheral fibres were present in the vicinity of the habenula perforata 2 weeks following deafness. This is consistent with many previous reports that have concluded that in aminoglycoside-induced deafness, SGN loss is secondary to loss of hair cells (e.g. Kohonen 1965; Leake-Jones and Vivion 1979; Hardie and Shepherd 1999; Glueckert et al. 2008). Furthermore, while evidence from the literature demonstrates widespread uptake of aminoglycosides by many cell types within the cochlea (Imamura and Adams 2003a; Heinrich et al. 2015), SGNs consistently exhibit low levels of uptake (Imamura and Adams 2003b; Heinrich et al. 2015), leading Imamura and Adams (2003b) to conclude that while aminoglycosides had a direct toxic effect on many cell types within the cochlea, only in the case of SGNs was the pathology secondary to the loss or damage to hair cells.

The Response of Schwann Cells to a Sensorineural Hearing Loss

Schwann cells continued to survive following the loss of their SGN, a finding that we have shown previously with S100 labelling in the deafened rat cochlea (Hurley et al. 2007). We observed numerous remnants of 'glial beds' where the membranous outline of a completely degenerated SGN remained. In addition, Schwann cells that had lost their SGN dedifferentiated and changed phenotype to a non-myelinating Schwann cell, consistent with our previous study where we reported a reduction in the level of staining for the myelin protein P0 but no change in the level of S100 (Hurley et al. 2007), as only myelinating Schwann cells express significant quantities of P0.

The dedifferentiated satellite Schwann cells observed in the present study assumed an 'astrocyte-like' morphology with numerous processes extending from the soma. These processes appeared to be sampling the extracellular environment, presumably searching for a new SGN target. Contact between the Schwann cell process and a residual SGN distorted the morphology of the soma (e.g. Fig. 11d–f).

Schwann cells within the peripheral nervous system are highly plastic and play a key role in axonal regeneration. Following peripheral nerve injury and loss of neural contact, myelinated Schwann cells rapidly dedifferentiate into a non-myelinating phenotype that upregulates repair factors, including neurotrophins, which are required for axonal regeneration. Once these dedifferentiated Schwann cells make contact with regenerating axons, they redifferentiate into a myelinating phenotype and restore nerve function (Glenn and Talbot 2013; Jessen and Mirsky 2016). This response to peripheral nerve injury is controlled by the transcription factor c-Jun which is upregulated on loss of neural contact and downregulates the myelinated Schwann cell phenotype in opposition to pro-myelin transcription factors (Parkinson et al. 2008; Arthur-Farraj et al. 2012). The role of specific transcription factors in controlling Schwann cell plasticity in the cochlea has yet to be determined.

Consistent with their role in the peripheral nervous system, we postulate that the dedifferentiated Schwann cell phenotype present in the deafened cochlea extends processors to contact residual SGNs in order to provide a reparative environment and to potentially remyelinate its host SGN. While we saw no clear evidence of remyelination in the present study, it is likely that the deafening technique used was so severe and widespread that any reparative influence of cochlear Schwann cells was minimal. While dedifferentiated Schwann cells in the peripheral nervous system can survive for long periods without

neural contact, their ability to support regenerating axons gradually diminishes (Jonsson et al. 2013); eventually, the denervated Schwann cells degenerate via $p75^{NTR}$-mediated apoptosis (Ahmad et al. 2015).

Clearing Cellular Debris Following Aminoglycoside Deafening

A feature of the present study was the lack of cellular debris during the course of the 12-week study. The only clear evidence of cell debris was a small number of degenerating SGN soma in the 6- and 12-week deafened cohorts (Fig. 8), implying that the cochlea possesses a rapid and efficient mechanism for phagocytosis. A variety of cochlear cell types are likely to contribute to this process including macrophages and microglia that are known to play an important role in clearing hair cell debris (Sato et al. 2010; Kaur et al. 2015; Sun et al. 2015; O'Malley et al. 2016; Fuentes-Santamaria et al. 2017). While we did not observe macrophages or microglia in the present study, their response to injury occurs rapidly with activation peaking from 1–10 days following the insult (Fuentes-Santamaria et al. 2017). Dedifferentiated Schwann cells play a major role in the phagocytosis of degenerating axons and myelin debris. Myelin breakdown occurs within 7 days of injury via Schwann cell autophagy (Gomez-Sanchez et al. 2015; Jessen and Mirsky 2016). This rapid clearing is consistent with the lack of myelin debris observed in the present study. Finally, macrophages attracted to the site in response to Schwann cell plasticity are also known to play an important role in myelin clearance (review: Scheib and Hoke 2013).

Clinical Significance

Post-mortem studies comparing SGN survival with a cochlear implant subject clinical performance in life have demonstrated a highly significant correlation between higher residual SGNs and improved word recognition scores in a given patient (Seyyedi et al. 2014). This result support attempts to promote survival of SGNs. Moreover, while contemporary cochlear implants typically use monopolar stimulation strategies that are known to excite wide regions of cochlea SGNs, new highly focused stimulation strategies are being developed; however, their efficacy is significantly reduced in cochleae with low or patchy SGN survival (Long et al. 2014; George et al. 2015).

Developing clinically relevant techniques for SGN rescue includes detailed knowledge of the ultrastructural and temporal response of SGNs in response to sensorineural hearing loss. It is equally important to study the cellular interactions during this degenerative process. This is particularly important for SGN/Schwann cell interactions given the important role Schwann cells play in peripheral nerve regeneration following injury.

Finally, there is evidence from both cochlear implant (Landry et al. 2013) and peripheral nerve stimulation studies (Singh et al. 2012) that electrical stimulation promotes neurite growth following neuronal injury. This approach may result in clinical significance if the electrical stimulus can be applied soon after injury in order to take advantage of the regenerative environment created by dedifferentiated Schwann cells. Such a therapeutic approach would be further enhanced by the simultaneous application of exogenous growth factors. Understanding the cellular interactions under these conditions will help drive the development of effective therapeutic interventions.

ACKNOWLEDGEMENTS

We are grateful for contributions made by Cong Ho, Anna Friedhuber, Marie Camilleri, Nicole Critch, Alison Neil, Stephen Asquith, Sarah Ellis, Maria Clarke, Prue Nielsen, and Ella Trang. The authors would like to acknowledge the funding support from the NIDCD (HHS-N-263-2007-00053-c and R01DC015031) and the NHMRC (GNT1064375). The Bionics Institute acknowledges the support it receives from the Victorian Government through its Operational Infrastructure Support Program.

COMPLIANCE WITH ETHICAL STANDARDS

The experimental procedures were approved by the Animal Research Ethics Committee of the Royal Victorian Eye and Ear Hospital in accordance with the National Institutes of Health Guidelines for the Care and Use of Laboratory Animals and conformed to the Code of Practice of the National Health and Medical Research Council of Australia.

Conflict of Interest The authors declare that they have no conflict of interest.

Role of Authors All authors had full access to all the data in the study and take responsibility for the integrity of the data and the accuracy of the data analysis. Study concept and design: AKW, RP, TGL, JBF, and RKS. Acquisition of data: AKW, RP, and TGL. Analysis and interpretation of data: AKW, RP, TGL, JBF, and RKS. Drafting of the manuscript: AKW, RP, TGL, JBF, and RKS. Critical revision of the manuscript for important intellectual content: AKW, RP, TGL, JBF, and RKS. Statistical analysis: AKW and TGL. Obtained funding: RKS and AKW. Study supervision: AKW.

REFERENCES

Adamo NJ, Daigneault EA (1973) Ultrastructural features of neurons and nerve fibres in the spiral ganglia of cats. J Neurocytol 2:91–103

Ahmad I, Fernando A, Gurgel R, Clark JJ, Xu L, Hansen MR (2015) Merlin status regulates p75(NTR) expression and apoptotic signaling in Schwann cells following nerve injury. Neurobiol Dis 82:114–122

Anniko M, Arnold W, Stigbrand T, Strom A (1995) The human spiral ganglion. Orl J Oto Rhino Laryngol Relat Spec 57:68–77

Arthur-Farraj PJ, Latouche M, Wilton DK, Quintes S, Chabrol E, Banerjee A, Woodhoo A, Jenkins B, Rahman M, Turmaine M, Wicher GK, Mitter R, Greensmith L, Behrens A, Raivich G, Mirsky R, Jessen KR (2012) c-Jun reprograms Schwann cells of injured nerves to generate a repair cell essential for regeneration. Neuron 75:633–647

Atkinson PJ, Wise AK, Flynn BO, Nayagam BA, Hume CR, O'Leary SJ, Shepherd RK, Richardson RT (2012) Neurotrophin gene therapy for sustained neural preservation after deafness. PLoS One 7:e52338

Bohne BA, Harding GW (1992) Neural regeneration in the noise-damaged chinchilla cochlea. Laryngoscope 102:693–703

Bohne BA, Harding GW, Nordmann AS, Tseng CJ, Liang GE, Bahadori RS (1999) Survival-fixation of the cochlea: a technique for following time-dependent degeneration and repair in noise-exposed chinchillas. Hear Res 134:163–178

Brown MC (1987a) Morphology of labeled efferent fibers in the guinea pig cochlea. J Comp Neurol 260:605–618

Brown MC (1987b) Morphology of labeled afferent fibers in the guinea pig cochlea. J Comp Neurol 260:591–604

Dodson HC (1997) Loss and survival of spiral ganglion neurons in the guinea pig after intracochlear perfusion with aminoglycosides. J Neurocytol 26:541–556

Fallon J, Ryugo DK, Shepherd R (2014) Consequences of deafness and electrical stimulation on the peripheral and central auditory system. In: Cochlear implants 3 handbook of clinical neurophysiology—disorders of peripheral and central Auditory processing: Thieme Publisher

Forge A (1985) Outer hair cell loss and supporting cell expansion following chronic gentamicin treatment. Hear Res 19:171–182

Forge A, Schacht J (2000) Aminoglycoside antibiotics. Audiol Neurootol 5:3–22

Fuentes-Santamaria V, Alvarado JC, Melgar-Rojas P, Gabaldon-Ull MC, Miller JM, Juiz JM (2017) The role of glia in the peripheral and central auditory system following noise overexposure: contribution of TNF-alpha and IL-1beta to the pathogenesis of hearing loss. Front Neuroanat 11:9

George SS, Wise AK, Fallon JB, Shepherd RK (2015) Evaluation of focused multipolar stimulation for cochlear implants in long-term deafened cats. J Neural Eng 12:036003

Gillespie LN, Zanin MP, Shepherd RK (2014) Cell-based neurotrophin treatment supports long-term auditory neuron survival in the deaf guinea pig. J Control Release:26–34

Gillespie LN, Clark GM, Bartlett PF, Marzella PL (2003) BDNF-induced survival of auditory neurons in vivo: cessation of treatment leads to an accelerated loss of survival effects. J Neurosci Res 71:785–790

Glenn TD, Talbot WS (2013) Signals regulating myelination in peripheral nerves and the Schwann cell response to injury. Curr Opin Neurobiol 23:1041–1048

Glueckert R, Bitsche M, Miller JM, Zhu Y, Prieskorn DM, Altschuler RA, Schrott-Fischer A (2008) Deafferentation-associated changes in afferent and efferent processes in the guinea pig cochlea and afferent regeneration with chronic intrascalar brain-derived neurotrophic factor and acidic fibroblast growth factor. J Comp Neurol 507:1602–1621

Gomez-Sanchez JA et al (2015) Schwann cell autophagy, myelinophagy, initiates myelin clearance from injured nerves. J Cell Biol 210:153–168

Hardie NA, Shepherd RK (1999) Sensorineural hearing loss during development: morphological and physiological response of the cochlea and auditory brainstem. Hear Res 128:147–165

Heinrich UR, Schmidtmann I, Strieth S, Helling K (2015) Cell-specific accumulation patterns of gentamicin in the guinea pig cochlea. Hear Res 326:40–48

Hurley PA, Crook JM, Shepherd RK (2007) Schwann cells revert to non-myelinating phenotypes in the deafened rat cochlea. Eur J Neurosci 26:1813–1821

Imamura S, Adams JC (2003a) Distribution of gentamicin in the guinea pig inner ear after local or systemic application. J Assoc Res Otolaryngol 4:176–195

Imamura SI, Adams JC (2003b) Changes in cytochemistry of sensory and nonsensory cells in gentamicintreated cochleas. J Assoc Res Otolaryngol, 4:196-218

Jessen KR, Mirsky R (2016) The repair Schwann cell and its function in regenerating nerves. J Physiol 594:3521–3531

Jonsson S, Wiberg R, McGrath AM, Novikov LN, Wiberg M, Novikova LN, Kingham PJ (2013) Effect of delayed peripheral nerve repair on nerve regeneration, Schwann cell function and target muscle recovery. PLoS One 8:e56484

Kaur T, Zamani D, Tong L, Rubel EW, Ohlemiller KK, Hirose K, Warchol ME (2015) Fractalkine signaling regulates macrophage recruitment into the cochlea and promotes the survival of spiral ganglion neurons after selective hair cell lesion. J Neurosci 35(45) :15050–15061

Kimura RS, Ota CY, Takahashi T (1979) Nerve fiber synapses on spiral ganglion cells in the human cochlea. Ann Otol Rhinol Laryngol Suppl 88:1–17

Knipper M, Bandtlow C, Gestwa L, Kopschall I, Rohbock K, Wiechers B, Zenner HP, Zimmermann U (1998) Thyroid hormone affects Schwann cell and oligodendrocyte gene expression at the glial transition zone of the VIIIth nerve prior to cochlea function. Development 125:3709–3718

Kohonen A (1965) Effect of some ototoxic drugs upon the pattern and innervation of cochlear sensory cells in the guinea pig. Acta Otolaryngol Suppl:1–70

Kujawa SG, Liberman MC (2009) Adding insult to injury: cochlear nerve degeneration after "temporary" noise-induced hearing loss. J Neurosci 29:14077–14085

Kujawa SG, Liberman MC (2015) Synaptopathy in the noise-exposed and aging cochlea: primary neural degeneration in acquired sensorineural hearing loss. Hear Res 330:191–199

Ladrech S, Guitton M, Saido T, Lenoir M (2004) Calpain activity in the amikacin-damaged rat cochlea. J Comp Neurol 477:149–160

Ladrech S, Wang J, Simonneau L, Puel JL, Lenoir M (2007) Macrophage contribution to the response of the rat organ of Corti to amikacin. J Neurosci Res 85:1970–1979

Landry TG, Fallon JB, Wise AK, Shepherd RK (2013) Chronic neurotrophin delivery promotes ectopic neurite growth from the spiral ganglion of deafened cochleae without compromising the spatial selectivity of cochlear implants. J Comp Neurol 521:2818–2832

Leake-Jones PA, Vivion MC (1979) Cochlear pathology in cats following administration of neomycin sulfate. Scan Electron Microsc 3:983–991

Leake PA, Hradek GT (1988) Cochlear pathology of long term neomycin induced deafness in cats. Hear Res 33:11–33

Leake PA, Hradek GT, Snyder RL (1999) Chronic electrical stimulation by a cochlear implant promotes survival of spiral ganglion neurons after neonatal deafness. J Comp Neurol 412:543–562

Leake PA, Hradek GT, Hetherington AM, Stakhovskaya O (2011) Brain-derived neurotrophic factor promotes cochlear spiral ganglion cell survival and function in deafened, developing cats. J Comp Neurol 519:1526–1545

Leake PA, Stakhovskaya O, Hetherington A, Rebscher SJ, Bonham B (2013) Effects of brain-derived neurotrophic factor (BDNF) and electrical stimulation on survival and function of cochlear spiral ganglion neurons in deafened, developing cats. J Assoc Res Otolaryngol 14:187–211

Lenoir M, Daudet N, Humbert G, Renard N, Gallego M, Pujol R, Eybalin M, Vago P (1999) Morphological and molecular changes in the inner hair cell region of the rat cochlea after amikacin treatment. J Neurocytol 28:925–937

Long CJ, Holden TA, McClelland GH, Parkinson WS, Shelton C, Kelsall DC, Smith ZM (2014) Examining the electro-neural interface of cochlear implant users using psychophysics, CT scans, and speech understanding. J Assoc Res Otolaryngol 15:293–304

McFadden SL, Ding D, Jiang H, Salvi RJ (2004) Time course of efferent fiber and spiral ganglion cell degeneration following complete hair cell loss in the chinchilla. Brain Res 997:40–51

McGuinness SL, Shepherd RK (2005) Exogenous BDNF rescues rat spiral ganglion neurons in vivo. Otol Neurotol 26:1064–1072

Menardo J, Tang Y, Ladrech S, Lenoir M, Casas F, Michel C, Bourien J, Ruel J, Rebillard G, Maurice T, Puel JL, Wang J (2012) Oxidative stress, inflammation, and autophagic stress as the key mechanisms of premature age-related hearing loss in SAMP8 mouse cochlea. Antioxid Redox Signal 16:263–274

Morrison D, Schindler RA, Wersall J (1975) A quantitative analysis of the afferent innervation of the organ of corti in guinea pig. Acta Otolaryngol 79:11–23

Nadol JB Jr, Young YS, Glynn RJ (1989) Survival of spiral ganglion cells in profound sensorineural hearing loss: implications for cochlear implantation. Ann Otol Rhinol Laryngol 98:411–416

O'Malley JT, Nadol JB, Jr., McKenna MJ (2016) Anti CD163+, Iba1+, and CD68+ cells in the adult human inner ear: normal distribution of an unappreciated class of macrophages/microglia and implications for inflammatory otopathology in humans. Otol Neurotol 37:99–108

Parkinson DB, Bhaskaran A, Arthur-Farraj P, Noon LA, Woodhoo A, Lloyd AC, Feltri ML, Wrabetz L, Behrens A, Mirsky R, Jessen KR (2008) c-Jun is a negative regulator of myelination. J Cell Biol 181:625–637

Pinyon JL, Tadros FS, Froud KE, Wong ACW, Tompson IT, Crawford EN, Ko M, Morris R, Klugmann M, Housley GD (2014) Close-field electroporation gene delivery using the cochlear implant electrode array enhances the bionic ear. Sci Transl Med 6

Puel JL, Pujol R, Tribillac F, Ladrech S, Eybalin M (1994) Excitatory amino acid antagonists protect cochlear auditory neurons from excitotoxicity. J Comp Neurol 341:241–256

Raphael Y, Kim YH, Osumi Y, Izumikawa M, (2007) Non-sensory cells in the deafened organ of Corti: approaches for repair. Int J Dev Biol 51(6-7):649-54

Richardson RT, O'Leary S, Wise A, Hardman J, Clark G (2005) A single dose of neurotrophin-3 to the cochlea surrounds spiral ganglion neurons and provides trophic support. Hear Res 204:37–47

Romero E, Cuisenaire O, Denef JF, Delbeke J, Macq B, Veraart C (2000) Automatic morphometry of nerve histological sections. J Neurosci Methods 97:111–122

Sato E, Shick HE, Ransohoff RM, Hirose K (2010) Expression of fractalkine receptor CX3CR1 on cochlear macrophages influences survival of hair cells following ototoxic injury. J Assoc Res Otolaryngol 11:223–234

Schecterson LC, Bothwell M (1994) Neurotrophin and neurotrophin receptor mRNA expression in developing inner ear. Hear Res 73:92–100

Scheib J, Hoke A (2013) Advances in peripheral nerve regeneration. Nat Rev Neurol 9:668–676

Seyyedi M, Viana LM, Nadol JB Jr (2014) Within-subject comparison of word recognition and spiral ganglion cell count in bilateral cochlear implant recipients. Otol Neurotol 35(8):1446-1450.

Shepherd RK, Javel E (1997) Electrical stimulation of the auditory nerve. I. Correlation of physiological responses with cochlear status. Hear Res 108:112–144

Shepherd RK, Coco A, Epp SB, Crook JM (2005) Chronic depolarization enhances the trophic effects of brain-derived neurotrophic factor in rescuing auditory neurons following a sensorineural hearing loss. J Comp Neurol 486:145–158

Singh B, Xu QG, Franz CK, Zhang R, Dalton C, Gordon T, Verge VM, Midha R, Zochodne DW (2012) Accelerated axon outgrowth, guidance, and target reinnervation across nerve transection gaps following a brief electrical stimulation paradigm. J Neurosurg 116:498–512

Spoendlin H (1975) Retrograde degeneration of the cochlear nerve. Acta Otolaryngol 79:266–275

Spoendlin H, Suter R (1976) Regeneration in the VIII nerve. Acta Otolaryngol 81:228–236

Spoendlin H, Schrott A (1989) Analysis of the human auditory nerve. Hear Res 43:25–38

Stankovic K, Rio C, Xia A, Sugawara M, Adams JC, Liberman MC, Corfas G (2004) Survival of adult spiral ganglion neurons requires erbB receptor signaling in the inner ear. J Neurosci 24:8651–8661

Strominger RN, Bohne BA, Harding GW (1995) Regenerated nerve fibers in the noise-damaged chinchilla cochlea are not efferent. Hear Res 92:52–62

Sun S, Yu H, Honglin M, Ni W, Zhang Y, Guo L, He Y, Xue Z, Ni Y, Li J, Feng Y, Chen Y, Shao R, Chai R, Li H (2015) Inhibition of the activation and recruitment of microglia-like cells protects against neomycin-induced ototoxicity. Mol Neurobiol 51:252–267

Tan J, Shepherd RK (2006) Aminoglycoside-induced degeneration of adult spiral ganglion neurons involves differential modulation of tyrosine kinase B and p75 neurotrophin receptor signaling. Am J Pathol 169:528–543

Terayama Y, Kaneko K, Tanaka K, Kawamoto K (1979) Ultrastructural changes of the nerve elements following disruption of the organ of Corti. II. Nerve elements outside the organ of Corti. Acta Otolaryngol 88:27–36

Toesca A (1996) Central and peripheral myelin in the rat cochlear and vestibular nerves. Neurosci Lett 221:21–24

van Loon MC, Ramekers D, Agterberg MJ, de Groot JC, Grolman W, Klis SF, Versnel H (2013) Spiral ganglion cell morphology in guinea pigs after deafening and neurotrophic treatment. Hear Res 298:17–26

Waaijer L, Klis SF, Ramekers D, Van Deurzen MH, Hendriksen FG, Grolman W (2013) The peripheral processes of spiral ganglion cells after intracochlear application of brain-derived neurotrophic factor in deafened guinea pigs. Otol Neurotol 34:570–578

Webster M, Webster DB (1981) Spiral ganglion neuron loss following organ of Corti loss: a quantitative study. Brain Res 212:17–30

Wise AK, Richardson R, Hardman J, Clark G, O'Leary S (2005) Resprouting and survival of guinea pig cochlear neurons in response to the administration of the neurotrophins brain-derived neurotrophic factor and neurotrophin-3. J Comp Neurol 487:147–165

Wise AK, Hume CR, Flynn BO, Jeelall YS, Suhr CL, Sgro BE, O'Leary SJ, Shepherd RK, Richardson RT (2010) Effects of localized neurotrophin gene expression on spiral ganglion neuron resprouting in the deafened cochlea. Mol Ther 18:1111–1122

Xu SA, Shepherd RK, Chen Y, Clark GM (1993) Profound hearing loss in the cat following the single co-administration of kanamycin and ethacrynic acid. Hear Res 70:205–215

Ylikoski J, Wersall J, Bjorkroth B (1975) Degeneration of neural elements in the cochlea of the guinea pig after damage to the organ of Corti by ototoxic antibiotics. Acta Otolaryngol (Stockh) Suppl 326:23–41

Ylikoski J, Pirvola U, Moshnyakov M, Palgi J, Arumae U, Saarma M (1993) Expression patterns of neurotrophin and their receptor mRNAs in the rat inner ear. Hear Res 65:69–78

Zilberstein Y, Liberman MC, Corfas G (2012) Inner hair cells are not required for survival of spiral ganglion neurons in the adult cochlea. J Neurosci 32:405–410

Zimmermann CE, Burgess BJ, Nadol JB Jr (1995) Patterns of degeneration in the human cochlear nerve. Hear Res 90:192–201